

Moderately-large-embedded-cluster approach to the study of local defects in solids. Vacancy and substitutional impurities in graphite

Cesare Pisani, Roberto Dovesi, and Paolo Carosso

Institute of Theoretical Chemistry, University of Turin, Via Pietro Giuria 5, I-10125 Torino, Italy

(Received 13 June 1979)

A method for studying local defects in solids is presented which is the development of an embedding approach first applied to the study of localized chemisorption. Its relationship with other embedding schemes is discussed, and it is shown that for its applicability larger cluster sizes are needed than customary in similar computations. This drawback is compensated by the characteristics of the embedding equations, which allow the method to be easily implemented starting from standard quantum-chemistry programs, and the self-consistent solution to be reached following well-tested procedures. A study of the isolated vacancy and of substitutional boron and nitrogen impurities in a monolayer of graphite is used to illustrate the method.

I. INTRODUCTION

The electronic structure of systems exhibiting translational symmetry except for a local defect is currently investigated using a number of different techniques (see, for example, Refs. 1-9 and references therein). This variety of approaches largely reflects the different kinds of physical properties that are under study. If short-range phenomena induced by the presence of the defect are considered, attention can be focussed on the defect itself and its close surroundings, provided, however, that proper boundary conditions are satisfied. So it is not surprising that calculations performed on isolated clusters¹⁰⁻¹¹ are critically dependent on the symmetry of the cluster and exhibit slow convergency with respect to its size. In fact, the number of dangling bonds increases with cluster size, and the incorrect behavior of the wave function at the boundary is likely to deeply affect the electronic properties of the solution near the defect itself. On the contrary, the embedding approach to the problem^{3,13-22} making explicit reference to the wave function for the unperturbed host solid to define the boundary conditions, correctly describes the asymptotic behavior of the solution. This technique has become particularly important in the last years, due also to the fact that sophisticated calculations of the electronic structure of periodic systems are becoming commonplace.

The aims of the present work are: (i) to illustrate, in a more general formulation, the embedding scheme recently presented by one of us (Ref. 19, hereafter referred to as I) and to compare the underlying assumptions with those of other embedding approaches; (ii) to check the validity of those assumptions in some typical cases; (iii)

to apply the theory to the study of some bulk defects of graphite. In Secs. II and III the first point is discussed and the fundamental embedding equations are derived. It is shown that our method's results are particularly effective when a basis set of atomic orbitals is used. In fact, in that case, the problem can be solved by performing conventional quantum-chemistry linear combination of atomic orbitals-molecular orbital (LCAO-MO) calculations within a cluster surrounding the defect. The correct connection of the cluster to the rest of the solid is obtained when redefining the density matrix at each cycle during the self-consistency process: to this purpose, use is made of energy-dependent coupling matrices which can be calculated once for all since they only depend on the solution for the unperturbed crystal. The conditions that must be satisfied for the validity of our simple scheme are more exacting than those underlying most other embedding techniques, which only require the perturbation to be practically zero outside the embedded cluster. In our case, the cluster must also comprise a connection zone surrounding the perturbed area. Therefore, the ease of solution and the computational speed that are warranted by the use of well-assessed programs and procedures are paid for by the necessity of using larger cluster sizes than is customary in similar computations; in this sense, our method characterizes itself as a "moderately-large-embedded-cluster" (MLEC) approach. On the other hand, due to the size of the cluster where the self-consistent computation is performed and to the structure of the computation itself, it is possible to calculate quantities that are critically dependent on the structure of the density matrix, in particular, the energy associated with the formation of the defect, a quantity which is beyond

the reach of ordinary schemes.

In Sec. IV some computational aspects of the MLEC method are examined and the fundamental problem of how large the local cluster must be for meaningful results to be obtained is discussed.

Concerning the applications of the theory, in paper I a preliminary study of hydrogen chemisorption on a monolayer of graphite had been presented. Here the same solid is used to test the efficiency of the method in treating more perturbing defects, namely, an isolated vacancy (Sec. V) and substitutional impurities of boron and nitrogen (Sec. VI). All calculations here reported have been performed in a CNDO approximation.²³ The reason for this choice is discussed in I; in particular, the extension of the method from CNDO to *ab initio* Hartree-Fock (HF)-LCAO formulations is straightforward and work in this direction is in progress.^{24,25}

II. THE GENERAL EMBEDDING EQUATIONS

A common feature of all existing embedding schemes is to project out of the vector space of the electron states of the system a local or "cluster" subspace of finite dimensions; we shall denote by C the set $\{\gamma_m\}$ of basis functions spanning this subspace and by $D \equiv \{\delta_m\}$ a complementary set of functions, which, broadly speaking, define the defective or indented solid. The meaning of the above partition will be clarified by the assumptions (a) and (b) to follow.

For ease of notation we shall use, throughout this work, the symbol Q to denote $G^{-1}(\epsilon)$, G being the representation of the Green's operator in the basis set $C \cup D$, that is:

$$\begin{pmatrix} Q_C & Q_{CD} \\ Q_{DC} & Q_D \end{pmatrix} \equiv Q(\epsilon) = (\epsilon + i0)S - H. \quad (1)$$

Here H is the Hamiltonian matrix for the perturbed system and S the overlap matrix. From $Q(\epsilon)G(\epsilon) = I$ one obtains, for each energy ϵ :

$$\begin{aligned} Q_C G_C + Q_{CD} G_{DC} &= I_C, \\ Q_{DC} G_C + Q_D G_{DC} &= 0, \end{aligned} \quad (2)$$

whence, by solving for G in the second row and substituting in the first one:

$$(G_C)^{-1} = Q_C - Q_{CD}(Q_D)^{-1}Q_{DC}. \quad (3)$$

In the same way the matrix $Q^f(\epsilon) = (\epsilon + i0)S - H^f$ can be defined for the free or unperturbed system. The local character of the set C corresponding to the short spatial range of the perturbation¹³⁻¹⁵ can now be formally introduced by the assumption that the perturbation potential V has nonzero matrix elements in the C set only:

$$V = H - H^f = Q^f - Q = \begin{pmatrix} V_C & 0_{CD} \\ 0_{DC} & 0_D \end{pmatrix}. \quad (4)$$

This equation is at the basis of all existing embedding calculations and will be referred to as assumption (a). From Eqs. (3) and (4) it follows:

$$(G_C)^{-1} = Q_C - Q_{CD}^f(Q_D^f)^{-1}Q_{DC}^f \quad (5)$$

which are the embedding equations as used, for example, by van Santen and Toneman.¹⁸ Equation (5) may be put into a different form by subtracting the corresponding equations for the unperturbed system; we then have equivalently:

$$\begin{aligned} (G_C)^{-1} &= (G_C^f)^{-1} - V_C, \\ G_C &= [(G_C^f)^{-1} - V_C]^{-1}, \\ G_C &= (I_C - G_C^f V_C)^{-1} G_C^f. \end{aligned} \quad (6)$$

One or another of the equivalent formulas (6) have been used by most authors.^{14-18,20-22} A more general formula has been proposed by Gunnarsson and Hjelmberg²⁰ starting from the only assumption that $V_D = 0$; however their applications are based on Eqs. (6). Equations (5) or (6) effectively confine the problem within the cluster C , once the solution for the free solid is known. In principle, they must be solved self-consistently because the Hamiltonian matrix H_C , hence also Q_C , generally depends on the density matrix P_C , which in turn is related to G_C by the relationship:

$$P_C = -\frac{1}{\pi} \text{Im} \int_{-\infty}^{\epsilon_F} G_C(\epsilon) d\epsilon, \quad (7)$$

where ϵ_F is the Fermi energy for the unperturbed system. Starting from a trial P_C matrix, Q_C and V_C are defined and $G_C(\epsilon)$ is evaluated at all energies by effecting matrix inversions according to Eqs. (5) and (6) (simpler procedures are possible in band gaps^{15,18}). The density matrix is recalculated according to Eq. (7), and so on up to convergence. In all this procedure, the main difficulty probably lies in the necessity of inverting, at each step of the self-consistent-field (SCF) stage, relatively large matrices that are often nearly singular in nature in correspondence to a high number of energy points; furthermore, the integration involved in Eq. (7) must be performed each time. The MLEC procedure, described in I, overcomes these difficulties, though at the cost of a further assumption; it is here presented in a more general formulation with respect to the previous derivation.

If we define, for each energy, a matrix J_C in the set C :

$$J_C(\epsilon) = Q_C^f(\epsilon)G_C^f(\epsilon), \quad (8)$$

our additional hypothesis, leading to the equations utilized in I, may be expressed as follows [assumption (b)]:

$$J_C(\epsilon)V_C = V_C. \quad (9)$$

Before deriving the consequences of this assumption, whose range of validity will be discussed in Sec. IV, let us discuss its meaning. To this purpose, using the well-known relationship between the Green's matrix and the density of states $\rho_m(\epsilon)$

$$G_{rm}^f(\epsilon) = P \int_{-\infty}^{+\infty} dt \frac{\rho_{rm}^f(t)}{\epsilon - t} - i\pi \rho_{rm}^f(\epsilon), \quad (10)$$

we can express more explicitly the elements of J_C :

$$J_{ln}(\epsilon) = \sum_r^{(c)} \left(P \int_{-\infty}^{+\infty} dt \frac{(\epsilon S - H^f)_{lr} \rho_{rm}^f(t)}{\epsilon - t} - i\pi (\epsilon S - H^f)_{lr} \rho_{rm}^f(\epsilon) \right). \quad (11)$$

Note that the sum over r extends only to functions belonging to the cluster C . Using the definitions:

$$\alpha_{ln}(\epsilon) = \sum_r^{(c)} (\epsilon S - H^f)_{lr} \rho_{rm}^f(\epsilon), \quad (12)$$

$$d_{ln} = \sum_r^{(c)} \int_{-\infty}^{+\infty} d\epsilon S_{lr} \rho_{rm}^f(\epsilon),$$

Eq. (11) becomes

$$J_{ln}(\epsilon) = P \int_{-\infty}^{+\infty} dt \frac{\alpha_{ln}(t)}{\epsilon - t} + d_{ln} - i\pi \alpha_{ln}(\epsilon). \quad (13)$$

Suppose now we can define, within C , a subset of central functions as distinguished from the complementary subset of border functions. The distinction is based on the fact that in Eqs. (12), if either l or n corresponds to the central region, the sums over r can be formally extended to the complete set $C \cup D$ without appreciable consequences. In this case, as is easily seen,¹⁹ it would result $\alpha_{ln} = 0$ and $d_{ln} = \delta_{ln}$. Hence, the structure of J_C would be as follows:

$$J_C(\epsilon) = \begin{pmatrix} I & 0 \\ 0 & X \end{pmatrix}. \quad (14)$$

The nonzero diagonal block denoted by X refers here to indices l and n both corresponding to the border region. Since by definition J_C becomes the unit matrix in the limit when C coincides with the whole basis set, the border region may be looked at as a connection zone between the central region and the defective solid. If J_C has the structure described by Eq. (14), for Eq. (9) to be true it is now sufficient to hypothesize that V is different from zero in the central region only.

In summary, it is seen that assumption (b) at the basis of the MLEC scheme corresponds to the requirement that the cluster C comprises a border region where the perturbation potential is already very small and where the connection of the cluster with the defective solid is established. In Sec. IV it will be discussed how large the local cluster must be for Eq. (9) to be an acceptable approximation. By assuming its validity we have, also using Eqs. (4), (8), and (6):

$$\begin{aligned} Q_C &= Q_C^f - V_C = Q_C^f - J_C V_C = J_C (J_C^{-1} Q_C^f - V_C) \\ &= J_C ((G_C^f)^{-1} - V_C) = J_C (G_C)^{-1}, \end{aligned} \quad (15)$$

whence:

$$G_C(\epsilon) = (Q_C(\epsilon))^{-1} J_C(\epsilon) \equiv \bar{G}_C(\epsilon) J_C(\epsilon). \quad (16)$$

Equation (16) is the fundamental equation for the MLEC approach. Its essential advantage with respect to Eqs. (5) or (6) is that the problem is here effectively factorized into a standard diagonalization within the cluster and into matrix multiplications. In fact, if $\bar{A} = \{\bar{a}_{mi}\}$ and $\bar{E} = \{\bar{e}_i \delta_{ij}\}$ are the solutions of the eigenvalue problem:

$$\begin{aligned} H_C \bar{A} &= S_C \bar{A} \bar{E}, \\ \bar{A}^t S_C \bar{A} &= I_C, \end{aligned} \quad (17)$$

it immediately results, assuming the basis set to be real:

$$\begin{aligned} \bar{G}_{mi}(\epsilon) &= [Q_C(\epsilon)]_{mi}^{-1} \\ &= \sum_i \bar{a}_{mi} \bar{a}_{ii} \left[P \frac{1}{\epsilon - \bar{e}_i} - i\pi \delta(\epsilon - \bar{e}_i) \right]. \end{aligned} \quad (18)$$

Here, P stands for "principal part of." By combining Eqs. (16), (18), (13), and integrating up to the Fermi level according to Eq. (7), we obtain:

$$\begin{aligned} P_{mn} &= -\frac{1}{\pi} \int_{-\infty}^{\epsilon_F} d\epsilon \sum_i^{(c)} [\text{Im}(\bar{G}_{mi}) \text{Re}(J_{ln}) \\ &\quad + \text{Re}(\bar{G}_{mi}) \text{Im}(J_{ln})] \\ &= \sum_{i,i} \bar{a}_{mi} \bar{a}_{ii} \left(\int_{-\infty}^{\epsilon_F} d\epsilon P \int_{-\infty}^{+\infty} dt \frac{\alpha_{ln}(t)}{\epsilon - t} \delta(\epsilon - \bar{e}_i) \right. \\ &\quad \left. + \int_{-\infty}^{\epsilon_F} d\epsilon d_{ln} \delta(\epsilon - \bar{e}_i) \right. \\ &\quad \left. + P \int_{-\infty}^{\epsilon_F} d\epsilon \frac{\alpha_{ln}(\epsilon)}{\epsilon - \bar{e}_i} \right) \\ &= \sum_{i,i} \bar{a}_{mi} \bar{a}_{ii} M_{ln}(\bar{e}_i), \end{aligned} \quad (19)$$

with

$$M_{ln}(e) = \begin{cases} d_{ln} - \int_{\epsilon_F}^{\infty} dt \frac{\alpha_{ln}(t)}{(t-e)} & (e < \epsilon_F) \\ \int_{-\infty}^{\epsilon_F} dt \frac{\alpha_{ln}(t)}{(t-e)} & (e > \epsilon_F). \end{cases} \quad (20)$$

It is seen that the matrices $M(e)$, play the role of coupling matrices between the cluster and the indented solid. As shown in I, the dependence on energy of these matrices is very smooth except for a discontinuity at the Fermi level. When they have been calculated once for all according to Eqs. (20) and (12) from the solution of the free solid, the defect problem becomes relatively simple. In fact, knowledge of the pseudoeigenvectors \bar{A} , which are obtained by conventional diagonalization procedures, allows the reconstruction of the density matrix by matrix multiplications [Eq. (19)] and, in turn, the redefinition of the Hamiltonian matrix H_C . This procedure can be carried on to self-consistency and all quantities of interest can be calculated, in particular, the differential energy associated with the defect, as shown in I. Also note that the same M matrices can be used to study a variety of defects of a given solid, provided the size of the cluster is adequate for the basic assumptions to be acceptable.

III. REFORMULATION OF THE EMBEDDING SCHEMES IN AN ATOMIC-ORBITAL BASIS

Actual embedding calculation are largely characterized by the basis set that is used to represent operators and wave functions. With few exceptions, notably the computations by Gunnarssen and Hjelmberg concerning the chemisorption of hydrogen on free or nearly free electron systems,²⁰ a basis set of atomic orbitals (AO) is usually chosen. Not only has the use of such sets met with unrivalled successes in the study of molecular systems, but it is spreading as a suitable and economical choice in the solution of a variety of solid-state problems.^{26,27} In order to exploit such a basis at its best, center, type, and scale factors of each orbital must be chosen in a very specific way for each particular problem. So, different sets should be employed for the unperturbed and the perturbed solid (see Fig. 1). In

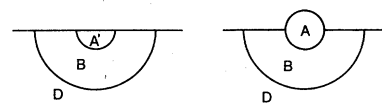


FIG. 1. Scheme for the partition of the basis set. To the left: the unperturbed solid; to the right: the embedded defect.

both cases a set $D = \{\delta_i\}$ of atomic orbitals is used to represent the defective solid, while two different sets $A' \cup B$ and $A \cup B$ are used to represent the local region where the perturbative Hamiltonian is different from zero. The meaning of the sets $A = \{\alpha_i\}$ and $A' = \{\alpha'_i\}$ is better clarified in Table I with reference to four typical embedding problems. The set $B = \{\beta_i\}$ comprises in both cases AO's of atoms surrounding the defect region; its extension is adjusted so as to justify the assumptions introduced in Sec. II as will soon become clear.

When trying to extend the use of the embedding equations that have just been derived to the case where an AO basis is adopted, care is required because it was assumed in Sec. II that the same basis set could be used for both the free and the perturbed solid, which is no more the case. A way out of this difficulty lies in the extensive application of an artifice introduced by Bernholc *et al.*¹⁵ in the study of vacancies in silicon, allowing the definition of a common set $C = A' \cup A \cup B$. Essentially, the artifice consists in adding some functions to a given basis set for representing a Hamiltonian operator, but in preventing them from contributing to the ground state by assigning them high and positive energy values. So, for instance, if we define $H_{\alpha\alpha}^f = E \gg \epsilon_F$, α being a general function belonging to A , the solution for the unperturbed system in the set $A' \cup B \cup D$ is the same as it is in the set $A' \cup A \cup B \cup B$. A symmetric procedure is adopted for the perturbed system. The advantage that is so gained is that it is now possible to define a difference V matrix as before. If it is assumed V

TABLE I. Examples of A' and A sets for several embedding problems.

Problem	Set A'	Set A
Vacancy	AO's of missing atoms	...
Substitutional impurity	AO's of substituted atom	AO's of impurity atom
Chemisorption of a molecule with no relaxation	...	AO's of atoms in the molecule
Formation of a surface molecule A-S, with displacement of the atom S, belonging to the adsorbing solid, from its free solid position	AO's of undisplaced S atom	AO's of A and AO's of S at its new position

to be zero in the subsets BD , AD and D [assumption (a')], it can be shown that all formal developments may be repeated as in Sec. II (see Appendix A) and Eqs. (6) become:

$$\begin{aligned} \begin{pmatrix} G_A & G_{AB} \\ G_{BA} & G_B \end{pmatrix} &= \begin{pmatrix} Q_A & Q_{AB} \\ Q_{BA} & (G_C^f)_B^{-1} - V_B \end{pmatrix}^{-1} \\ &= \begin{pmatrix} Q_A & Q_{AB} \\ Q_{BA} & Q_B - Q_{BD}^f (Q_D^f)^{-1} Q_{DB}^f \end{pmatrix}^{-1}. \end{aligned} \quad (21)$$

To define $(G_C^f)_B^{-1}$ in the above equation, first construct the Green matrix G^f for the unperturbed system, then invert the submatrix corresponding to the subset $A' \cup B$ and take its B portion. Of course, such a procedure must be repeated for each energy.

Equations (21) encompass a number of different approaches; three of them are briefly recalled here by way of example.

In Grimley's pioneering work on chemisorption of hydrogen on an ideal cubic solid,^{3,17} the set A is reduced to a single atomic orbital, corresponding to the adsorbed hydrogen atom; the set B also comprises a single AO, that of the underlying metal atom, and A' is empty. In this case, the inversion of the two-by-two matrix may be algebraically worked out for each energy value. The resulting equations are solved to self-consistency by recalculating at each cycle the P matrix in cluster C through numerical integration of the imaginary part of G_C up to the Fermi level [see Eq. (7)]. The only formal difference is that here the perturbing potential V_B also includes the change in Coulomb repulsion energy of electrons on atom B , whereas in Ref. 17 this term was added separately, since it had not been included in V_B .

Van Santen and Toneman¹⁸ use the second of Eqs. (21) in the study of chemisorption at the end of a linear chain at atoms. Again, the set A' is empty, but B now includes a number of AO's near the end of the chain. The self-consistent solution of their final equations indeed appear very difficult except for such simple problems as the one they use for illustration of the method. In particular, their one-electron effective Hamiltonian includes a term, denoted by Λ , which is energy dependent, so it is not true that finding the coefficients for surface resonances is reduced to solving an eigenvalue problem.

In the work on vacancies by Bernholc *et al.*¹⁶ the set A' coincides with the missing atom, and the set A is empty. So, Eq. (21) is reduced to $G_B^{-1} = (G_C^f)_B^{-1} - V_B$, which must be solved to self-

consistency in a cluster which extends over the region where $V_B \neq 0$. Of course, this involves again performing the matrix inversion at a number of energy point and integrating up to the Fermi level. Incidentally, note that for applicability of the embedding equations to this problem, it is not required that the interaction between the missing atom and the defective solid is negligible in the unperturbed solid, since this hypothesis is not comprised in assumption (a).

Following the same procedure that was adopted to derive Eq. (21) it is possible to generalize Eq. (16) for application to cases where A , or A' or both are nonempty. To this purpose, in addition to previous assumptions, one must further hypothesize that the border region of cluster C , as defined in Sec. II, is entirely confined within B [assumption (b')], so that Eq. (9) is still satisfied. In this case we obtain:

$$\begin{pmatrix} G_A & G_{AB} \\ G_{BA} & G_B \end{pmatrix} = \begin{pmatrix} \bar{G}_A & \bar{G}_{AB} J_B \\ \bar{G}_{BA} & \bar{G}_B J_B \end{pmatrix} \quad (22)$$

where we have defined [see Eq. (8)]: $J_B = Q_{BA}^f G_{A'B}^f + Q_{BB}^f G_{BB}^f$. The MLEC Eqs. (12), (19), and (20) are still valid. Just note that in those expressions the index r runs over the set $A' \cup B$, the index m runs over $A \cup B$ and the indices n and l over B . When n belongs to set A , we can no longer define P_{mn} according to Eq. (19), but we have simply, from Eq. (22):

$$P_{mn} = \sum_{i(\bar{\epsilon}_i < \epsilon_F)} \bar{a}_{mi} \bar{a}_{ni}.$$

The P matrix defined in this way is symmetric, as it should be, only if assumption (b') is strictly satisfied; in practice this is not exactly the case. In order to solve this difficulty, in paper I we calculated only the lower half of the P matrix and defined $P_{mn} = P_{nm}$ for $n > m$. An alternative scheme consists in using for the density matrix the symmetrized expression $\frac{1}{2}(P + \bar{P})$. We have used the two procedures in a number of applications, the results are quite comparable, except for the fact that convergency was reached more easily following the second procedure, which is currently adopted.

IV. CHOICE OF THE CLUSTER SIZE AND COMPUTATIONAL PROBLEMS

The general computational scheme has been described in I in some detail; we shall, therefore, concentrate our attention on the most critical aspects of the method and its implementation. The monolayer of graphite is taken as a reference system for the present discussion; in Fig. 2

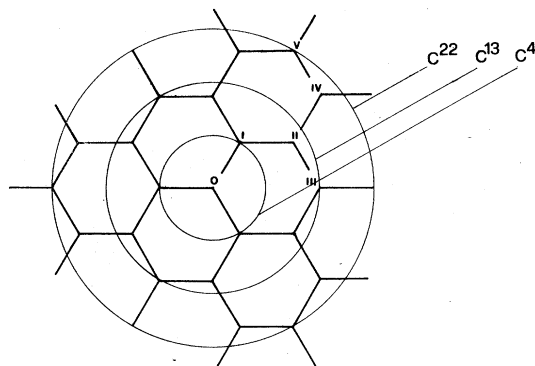


FIG. 2. Identification of C clusters of different sizes in the graphite lattice and numeration of atoms according to their distance from the central atom in the cluster.

clusters of different sizes are represented and atomic positions are identified for subsequent reference.

The first problem is to evaluate what size the C cluster must have for assumption (a), (a') and (b), (b') to be acceptable. In order to ascertain the spatial range of the perturbation, we have considered a self-consistent MLEC calculation concerning a vacancy at the center of a C_{22} cluster. In Table II standard deviations between H^f and H are reported for different atomic blocks. For comparison, the root-mean-square values of H^f on diagonal atomic blocks and on blocks relating an atom to its first, second, and third neighbors are 195, 260, 55, 27, respectively, in the same units as used in Table II. It is seen that the perturbative Hamiltonian V gradually decreases towards the border of the cluster. No net distinction, as is known to occur in free and nearly free electron systems, exists between a highly perturbed zone and an outer region where electrostatic forces are screened with high effectiveness. A comparable extent of the perturbation induced by a vacancy in graphite is reported

TABLE II. Root-mean-square values for some atomic blocks of the perturbation matrix for a vacancy in graphite. Energies are in units of 0.001 a.u. The atoms here considered are those labeled with the same symbols in Fig. 2.

Atom	I	II	III	IV	V
I	60	12	11	7	7
II		24	4	4	2
III			26	2	1
IV				12	4
V					6

by Zunger and Englman.⁸ Also note that diagonal elements of the V matrix are appreciably higher than out-of-diagonal ones; this feature can be explained in terms of the assumed orthogonality of AO's in CNDO schemes, preventing external Coulomb fields from affecting nondiagonal terms. If one takes, rather arbitrarily, 0.01 a.u. as the value below which the perturbation is considered negligible, from Table II and from data referring to other defects, it results that for a C_{13} cluster assumption (a') is roughly satisfied.

It is even more difficult to unambiguously establish the size of the central region, as defined in the discussion leading to Eq. (15). In fact, the extent of this region not only is related to the size of the C cluster, but is also critically dependent on energy. In the case of a C_{22} cluster, the structure of $J_C(\epsilon)$, as represented in Eq. (14) is satisfactorily reproduced in the average by defining the central region as comprising two shells of neighbors of the central site. However, at certain energy points, some elements which should be zero, especially those far from the diagonal, are found to assume values up to 0.1. A safe choice would then be to take the central region as extending only to one shell of neighbors of the central atom for MLEC calculations performed with C_{22} embedded clusters.

On combining this result with the previous one concerning the size of the region where V differs from zero, we could conclude that assumption (a') and (b') are satisfied only in a rather crude way when a C_{22} embedded cluster is used to study bulk defects in graphite. On the other hand, when considering integrated quantities such as the density matrix, the effects related to failures of Eq. (9) at specific energy points are smoothed out. For example, the coupling M matrices which result from an integration similar to the one involved in the definition of J , but with the exclusion of singularities, possess the structure exhibited in Eq. (14), with the border region effectively confined to the shells of atoms with dangling bonds towards the indented solid, that is, atoms labelled IV and V in Fig. 2 for a C_{22} cluster (see also paper I for a C_{13} cluster).

To test the validity of assumption (b') and the soundness of the computational scheme, we have considered a quite simple case for which the correct solution is known *a priori*, that is, the substitution of an atom of the solid with itself. If all assumptions are correct, the unperturbed solid solution should be found again. This is not the same calculation as performed in I: there, it has been simply checked that in the absence of any perturbation (A and A' both empty), the embedded cluster calculation furnished the same results as

the unperturbed solid. Here A and A' both contain the self-substituted atom. Hence the correction described by Eq. (19) is not applied to AO's belonging to that atom; this should not matter only if that atom is within the central region, where border effects are not felt.

The results are shown in Table III. It is seen that the electronic structure of the MLEC solution is very near to the unperturbed situation already for the C_{13} cluster. On the contrary, the isolated C_{22} cluster solution exhibits high discrepancies with respect to infinite graphite even at the center of the cluster, of the same order as those encountered in the C_4 embedded cluster. This is confirmed from the energy data that are given in the last two rows. For embedded-cluster calculations, ΔE_b was calculated according to the expression

$$\Delta E_b = -\frac{1}{2} \text{Tr}^C (P(F+H) - P'(F'+H')),$$

which corresponds to assuming ΔP to be zero outside the cluster. E_b was then obtained by subtracting ΔE_b from E_b^f . Concerning the isolated cluster, E_b represents the mean binding energy per atom in the cluster.

In conclusion, these calculations support the hypothesis that, in a C_{22} embedded cluster, the site at the center and probably its nearest neighbors are well beyond the influence of border effects.

Once the cluster size has been chosen the $M(e)$ matrices can be calculated owing Eq. (20), from the solution for the unperturbed solid. In princi-

ple, in order to calculate P_{mn} according to Eq. (19), one should calculate those matrices in correspondence to all eigenvalues e_i as they come out during the self-consistent step. In practice, the M matrices are sampled once and for all at a limited number of regularly spaced energy points, and an interpolation procedure is used to reconstruct them at any desired e_i value. Since the dependence of M on energy is luckily very smooth, as shown in I, a simple interpolation procedure according to expression:

$$M_{\sigma\nu}(e) = \sum_{j=1}^3 [a_{j,\sigma\nu}(e - \epsilon_j)^{-1} + b_{j,\sigma\nu}(e - \epsilon_j)^{-2}].$$

was found to reproduce the correct M values to about six significant figures. Different parameters $a_{j,\sigma\nu}^{\pm}$, $b_{j,\sigma\nu}^{\pm}$, and ϵ_j^{\pm} must of course be used according to whether ϵ is below or above ϵ_F . The nonlinear parameters ϵ_j^{\pm} are obtained by trial and error, but their choice is not very critical provided $\epsilon_j > \epsilon_F$ if $e < \epsilon_F$ and vice versa.

After the ϵ_j values have been determined, the a and b parameters are calculated by a linear least-squares procedure. In this way, the whole information concerning the M matrices is economically summarized into twelve matrices A_j^{\pm} , B_j^{\pm} , and six nonlinear parameters ϵ_j^{\pm} .

A critical point will be finally examined in the present section, i.e., what computational devices must be employed in order to increase the speed of convergency and to reduce the risk of diver-

TABLE III. Self-substitution of a carbon atom in graphite. ΔP^0 is the root-mean-square deviation of the density matrix on central atom from unperturbed graphite values. For each shell of neighbors of central site, according to the numeration of Fig. 2, the electron distribution is described by providing the hybridization ratio $h^{(n)}$, that is the ratio between $p_x + p_y$ and s -orbital population, plus the population $P_z^{(n)}$ on the π orbital p_z . E_b^f , binding energy of substituted atom and ΔE_b , its difference from the binding energy of carbon in graphite, are calculated as described in the text.

Cluster	C_4	C_{13}	C_{22}	∞	Isolated C_{22}
ΔP^0	0.024	0.013	0.004	0.0	0.024
h^0, P_z^0	2.07, 0.92	1.98, 1.01	2.06, 1.00	2.06, 1.00	1.99, 1.08
h^I, P_z^I	1.85, 1.06	2.06, 1.00	2.05, 1.00	2.06, 1.00	1.90, 1.02
h^{II}, P_z^{II}	...	2.05, 1.00	2.06, 1.00	2.06, 1.00	1.98, 0.99
h^{III}, P_z^{III}	...	2.06, 1.00	2.06, 1.00	2.06, 1.00	1.31, 0.78
h^{IV}, P_z^{IV}	2.06, 1.00	2.06, 1.00	1.40, 1.09
h^V, P_z^V	2.06, 1.00	2.06, 1.00	1.73, 0.97
E_b (eV)	21.6	27.7	26.8	26.9	22.4
ΔE_b (eV)	-5.3	0.8	-0.1	...	-4.5

gencies during the self-consistent procedure. This is an important problem in many quantum-chemistry calculations, especially when infinite systems are considered; the simple trick of adding at each iterative step a fixed fraction α of the old density matrix to the new one multiplied by $(1 - \alpha)$ is often a way out of difficulties.^{22,28} In the present case, however, the risk of divergencies is enhanced by the fact that the electronic charge in the cluster is not fixed but is determined by the position of the Fermi level through Eq. (20). Therefore, when the self-consistent procedure is still far from convergency, charge instabilities may occur.²²

In order to quench them, we have chosen at each iteration the α mixing coefficient within a certain interval (0.3 to 0.8) so that the resulting P matrix corresponded as closely as possible to charge neutrality. This was, however, not sufficient, and an independent charge renormalization had to be effected. It was accomplished by multiplying the density matrix by a factor $(1 + f(\delta, i))$, where $f(\delta, i) = \delta - a_i \tan(\delta/a_i)$ is both a function of the fractional excess positive charge in the cluster $\delta = (Q^+ - Q^-)/Q^+$ and of the iterative cycle i , through a coefficient a_i . Initially, a_i is low (~ 0.001) with respect to usual δ values. Then $f \approx \delta$ and the correction is complete; gradually a_i is increased up to 0.1 which is much greater than δ , and f_i becomes practically zero; so, no correction is operated in the final stages of the computation. Using these precautions, convergency is usually reached within about fifteen iterations.

V. THE VACANCY IN A GRAPHITE MONOLAYER

The case of an unrelaxed vacancy was considered in four different approximations: MLEC calculations for C_{13} and C_{22} embedded clusters (in the following referred to as e_1 and e_2 , respectively), and the corresponding calculations for isolated clusters (i_1 and i_2). In all cases, the vacant site was at the center of the cluster. The results are shown in Tables IV and V.

The energy of extraction of a carbon atom from graphite is given first; it was obtained with reference to another calculation for a cluster of the same size but comprising the central carbon atom. In cases e_1 and e_2 the reference system was of course an embedded cluster; when calculating the extraction energy, it was assumed that changes in the density matrix in the defective solid as induced by the vacancy provided a negligible contribution to differential energy (see paper I for details). The values here reported are nearly four times as high as the experimental extraction energy which is estimated to be about

TABLE IV. MLEC and isolated cluster results for the vacancy in graphite. ΔE is the energy for extraction of a carbon atom from the lattice, $q^{(n)}$ is the net charge on the n th neighbor of central site (see Fig. 2), and $\Delta P^{(n)}$ are the corresponding rms deviations of the density matrix from unperturbed graphite values.

ΔE (eV)	Embedded cluster		Isolated cluster	
	$C_{13}(e_1)$ 46.0	$C_{22}(e_2)$ 49.1	$C_{13}(i_1)$ 40.8	$C_{22}(i_2)$ 50.9
q^I	-0.174	-0.151	-0.147	-0.044
q^{II}	0.107	0.052	0.120	0.077
q^{III}	-0.062	-0.029	-0.093	-0.237
q^{IV}	...	0.024	...	0.120
q^V	...	0.013	...	-0.113
ΔP^I	0.099	0.108	0.219	0.158
ΔP^{II}	0.046	0.022	0.194	0.039
ΔP^{III}	0.072	0.065	0.196	0.183
ΔP^{IV}	...	0.028	...	0.144
ΔP^V	...	0.005	...	0.080

13 eV, as obtained by summing the sublimation and vacancy formation energies (see Ref. 8 for a detailed discussion). Gross overestimations of binding energies, up to factors of 5, are known to occur in CNDO computations,^{23,28} even if the relative order of energies is usually meaningful.

An apparent convergency of the energies calculated according to the two procedures to a common value of about 50 eV is observed. This finding must probably be taken as fortuitous, not only

TABLE V. Populations of planar hybrid and π orbitals for C_{22} MLEC and isolated cluster calculations of the vacancy in graphite. h is defined as in Table III. Atoms are numbered as in Fig. 2.

Atom	Embedded cluster			Isolated cluster		
	sp^2	h	P_z	sp^2	h	P_z
I	1.199	1.486	1.104	1.052	1.294	1.212
	0.924			0.890		
	0.924			0.890		
II	0.992	1.984	0.973	1.064	1.910	1.020
	1.025			0.963		
	0.958			0.876		
III	0.987	2.009	1.164	0.865	1.587	0.703
	0.987			0.865		
	0.890			1.804		
IV	0.992	1.915	1.029	0.992	1.360	0.846
	0.993			0.933		
	0.962			1.109		
V	1.004	2.047	1.005	0.928	1.663	1.019
	1.004			0.926		
	0.974			1.238		

because the two isolated cluster calculations still exhibit large energy difference from each other, but also because analysis of the electronic structure seems to indicate that in isolated clusters of the size considered by us, border effects are still very important at the center of the cluster. Consider in fact, in the same Table IV, the net charges $q^{(n)}$ on different neighbors of the central site. At first sight, the general picture is the same in all cases: an appreciable charge builds up on the three atoms nearest to the vacancy (type I atoms) and charge oscillations propagate in subsequent shells of neighbors. However, while such oscillations are quenched in a relatively effective way in the case of the embedded clusters, in cases i_1 , i_2 the perturbation induced by the abrupt truncation at the external border clearly propagates throughout the cluster; this is even more evident if one considers $\Delta P^{(n)}$ values, which are the standard deviations of the first-order density matrix on each atom with respect to unperturbed solid values.

The anisotropy induced by the vacancy is best described in terms of hybrid AO's (see Appendix B). If pure sp^2 hybridization occurs, each hybrid orbital (HO) should contain one electron, and the hybridization ratio (h), defined as $(P_{xx} + P_{yy})/P_{ss}$ should be 2: in unperturbed graphite, according to our calculations, it is 2.058.

In Table V the results of such a population analysis are reported for the calculations e_2 and i_2 . For each atom the three HO's are numbered starting from the one, or the ones, pointing nearest to the vacant site. Note again that the discrepancies from the unperturbed solid situation decay rapidly towards the border of the cluster in case e_2 . The most interesting feature of this table concerns, however, the strong anisotropy of the electron distribution on type I atoms: the HO pointing toward the center has a population which is 1.3 times the population on the other HO's. This suggests that the bonds of the three atoms with their first neighbors are loosened in favor of a delocalized bond through the vacancy. This finding is in disagreement with Zunger and Englman's results.⁸

Those authors have performed an important series of computations, in an extended Hückel approximation, concerning graphite-type periodic structures containing regularly spaced vacant sites. They considered cells each containing 7, 17, 31, 49 carbon atoms surrounding a vacancy and studied the convergence of the electronic properties of the superlattice with respect to the size of the basic cell. Their more characteristic result was the appearance of a doubly degenerate singly occupied level of E' symmetry,

located in the pure π region, quite near to the Fermi level, and corresponding to crystalline orbitals spatially localized on the atoms surrounding the vacant site. As a consequence, on those atoms σ and π charges of 3.76 and 0.42 electrons were observed, which is a completely different picture from the one reported in Table V. According to the authors, their data indicate a migration of the π charge towards the nearest neighbors and stabilization of the corresponding C-C bond. This became more evident when allowing type I atoms to relax: the equilibrium structure corresponded to an appreciable displacement away from the vacant site, with a further enhancement of the bond population with neighboring atoms.

In order to further explore the different behavior of the two kinds of computations, we performed a study of symmetric relaxation about the vacancy. In a strict sense, according to the discussion of Sec. III, when considering this problem one should include the AO's of the three displaced atoms in the A set, while the same AO's, but centered at their unperturbed solid positions, should enter A' , together with the AO's of the central missing atom. A much larger cluster should, however, be needed in this case for assumptions (a') and (b') to hold true. Therefore, an intermediate scheme has here been adopted: the P matrix is modified according to Eq. (19) as though A' were confined to the missing atom, but the Hamiltonian is calculated by taking into account the new positions of the nuclei.

The results of these calculations are shown in Fig. 3 for the C_{22} embedded cluster. The equilibrium structure is seen to correspond to a slight displacement of the three atoms towards the center, by 0.04 Å, with a gain in energy of about 0.7 eV. Zunger and Englman, as shown in the same figure, have found a displacement of 0.05 Å in the opposite direction with a comparable

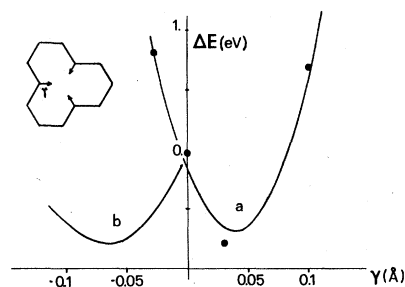


FIG. 3. Energy changes on symmetric relaxation of the three type I atoms about the vacancy. Curve a: best-fit parabola through the four points (full circles) calculated in the present work; curve b: results of Ref. 8.

gain in energy. A difference in calculated equilibrium bond lengths of 0.1 Å is not in itself surprising if one considers that the semiempirical scheme is not the same in the two cases.

On the other hand, on closer examination, the two calculations reveal more essential differences. We did not find any one-electron states that could unambiguously be related to Zunger's localized ring-shaped orbitals of symmetry E' . Rather, a well localized σ orbital of local $A1'$ symmetry is observed by us, corresponding to a through-vacancy bond. Its characteristics are shown in Fig. 4. Since it lies well below the Fermi energy, and also due to its localized character, the contribution of this molecular orbital to the density matrix according to Eq. (19) is practically unaffected by the coupling M matrices and may therefore be analyzed according to the usual schemes. It is seen that about half of the electronic population on this level is associated with the three type I atoms, the rest being essentially concentrated on the ring of their six nearest neighbors. The character of through vacancy bond orbital is apparent not only from the analysis of the coefficients $\bar{a}_{\mu i}$, but also from the fact that the level deepens and becomes more localized as the three atoms approach. It is this molecular orbital that characterizes the overall electronic structure of the system and makes it so different from Zunger's results.

This fundamental discrepancy cannot be traced back, in our opinion, to the different semiempirical approaches and to the calculation schemes that were adopted. A significant detail is possibly at the basis of this contradiction. In our calculation we did not force either the cluster to be neutral (see Sec. III), although it practically re-

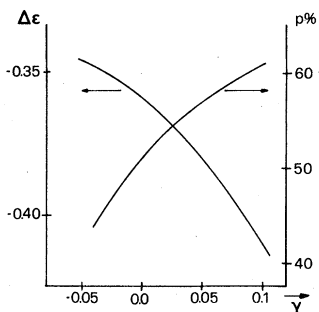


FIG. 4. Characterization of the localized molecular orbital corresponding to a through-vacancy bond. $\Delta\epsilon = \epsilon_i - \epsilon_F$ is the difference between the energy level associated to this orbital and the Fermi energy and is measured in a.u. p is the percentage of the electron population on this orbital (containing two electrons) that is localized on the three type I atoms. $\Delta\epsilon$ and p are reported as functions of the relaxation parameter γ defined in Fig. 3.

sulted to be so, nor imposed the population on the π system to be exactly one-third of the population of the σ system. In fact, we find the π electron charge in the cluster to be 0.8 electrons higher than that obtained by formally assigning one electron per p_z orbital. A corresponding defect of 0.8 electrons occurs in the σ system.

On the contrary, in Zunger and Englman's calculation the number of π and σ electrons was rigidly imposed, which led to two different Fermi levels for the two systems. According to our results, if a self-consistent estimation of the Fermi level had been effected by those authors, their defect level would have been practically unoccupied, with a significant alteration of their final results.

VI. SUBSTITUTIONAL IMPURITIES IN A GRAPHITE MONOLAYER

MLEC calculations of boron and nitrogen substitutional impurities in a graphite monolayer have been performed with C_{22} embedded clusters. In Tables VI and VII we report for these cases the same quantities as given in Tables IV and V for the vacancy. q^0 designates the net charge on the impurity atom. When comparing these data with the corresponding ones for the vacancy, one can first of all classify them in the order boron < nitrogen < vacancy, according to the amount and to the spatial extent of the alteration induced by the defect in the electronic structure of the host material. This sequence is also observed in the energies necessary for the reaction: $(S) + G \rightarrow G' + C$, S and C designating the impurity and carbon atom at infinity in their ground state (S is absent in the case of vacancy formation), G and G' graphite in its unperturbed and perturbed state. Again, not too much meaning should be attributed to absolute ΔE values as reported in

TABLE VI. C_{22} MLEC results for substitutional impurities in graphite. All symbols as in Table IV.

	Substitutional nitrogen	Substitutional nitrogen
ΔE (eV)	8.4	1.8
q^0	0.012	-0.138
q^I	0.078	-0.035
q^{II}	-0.008	0.009
q^{III}	0.004	-0.001
q^{IV}	-0.019	0.005
q^V	0.002	-0.002
ΔP^I	0.056	0.053
ΔP^{II}	0.014	0.011
ΔP^{III}	0.016	0.011
ΔP^{IV}	0.016	0.008
ΔP^V	0.007	0.007

Table VI: it is however gratifying that they are both positive and that boron impurities are much more stable than nitrogen ones, in agreement with the experimental findings of chemical impurities in natural graphite.²⁹

Atomic charges and population of hybrid orbitals exhibit a very symmetric behavior for boron and nitrogen impurities. This general structure can be interpreted in terms of the classical bond picture of the formation of impurity levels in semiconductors. Boron and nitrogen atoms fit into a pattern of σ trigonal bonds and delocalized π bonds by accepting and donating an electron, respectively. As a consequence, a center of negative and positive charge is created in the two cases, and a hole or an electron is loosely bound to the impurity. Of course, this interpretation should not be taken too literally due to the fact that graphite is a zero-gap semiconductor. On examination of the hybrid population reported in Table VII it appears that the charge rearrangement involves σ and π electrons to about the same degree: furthermore, in neither case is a single molecular orbital clearly recognizable as a donor or acceptor state, as are encountered, for example, in the study of impurities in diamond.¹⁰ It should also be remembered that all our calculations have concerned closed-shell configurations even for odd number of electrons in the neutral isolated cluster; an interesting development will be the extension of such calculations to open-shell

cases.

In conclusion, the realistic treatment of local perturbations in infinite periodic systems according to embedding procedures now appears to be a feasible though cumbersome undertaking. The problem has inherent difficulties which make impossible drastic shortcuts. Essentially, the spatial range of the perturbative Hamiltonian is not always very limited, and in all cases the region where the density matrix exhibits appreciable variations with respect to free-solid values involves some shells of neighbors round the defect. If one is not interested solely in properties strictly associated with the defect region, such as for instance the local density of states, but wants a description of the solution to a degree of precision as available from standard quantum-chemistry calculations, relatively large embedded clusters must be considered. In these cases the scheme here proposed appears accurate and simple enough; convergency problems in the self-consistent procedure have been overcome in all cases was considered. Specific storage requirements relative to memorization of the cluster-solid coupling matrices are not severe; the difference in the computing time, with respect to cluster calculations, is related to the reconstruction of the P matrix according to Eq. (19); this time is about the same as needed for diagonalization. With respect to a method of comparable accuracy, such as the treatment of periodic superlattices of large basic cells containing the defect, our method is undoubtedly faster because it embodies from the start all knowledge concerning the asymptotic solution.

More extended studies are required to assess the advantages that are gained in this way with respect to simple isolated cluster calculations; our tests seem to indicate that perhaps a factor of 2 in the number of atoms is needed in the latter case to reach, at the cluster center, an accuracy comparable to that provided by an embedded-cluster calculation.

ACKNOWLEDGMENT

This work was partially supported by the Italian Council of Research (CNR).

APPENDIX A

Consider for simplicity, an orthogonal basis. As explained in Sec. III we shall represent the operator $\hat{Q}^f = \hat{G}^{f-1}$ in the common basis $A' \cup A \cup B \cup D$ in the form:

TABLE VII. Populations of planar hybrid and π orbitals for C_{22} MLEC calculations of substitutional impurities in graphite. All symbols as in Table V.

Atom	Substitutional nitrogen			Substitutional boron		
	sp^2	h	P_z	sp^2	h	P_z
I	{0.816 1.053 1.053}	1.867	0.999	{1.188 0.941 0.941}	2.136	0.964
II	{1.011 1.003 0.985}	2.047	1.008	{0.984 1.008 1.000}	2.031	0.999
III	{0.988 0.988 1.053}	2.041	0.966	{1.010 1.010 0.959}	2.068	1.023
IV	{0.959 1.000 1.022}	2.016	1.038	{1.020 0.997 0.979}	2.030	0.999
V	{1.009 1.009 1.001}	2.057	0.977	{0.994 0.994 0.997}	2.035	1.018

$$Q^f(\epsilon) = \begin{pmatrix} F & 0 & F & F \\ 0 & \epsilon - E & 0 & 0 \\ F & 0 & F & F \\ F & 0 & F & F \end{pmatrix}_{A',A,B,D} \quad (\text{A1})$$

where $\epsilon - E$ stands shortly for $(\epsilon + i0 - E)I_A$, E is an energy much above the Fermi energy ϵ_F , and the submatrices F (free) are the same as the corresponding submatrices representing \hat{Q}^f in the natural basis $A' \cup B \cup D$. The Green matrices $(Q^f(\epsilon))^{-1}$ have of course no additional poles below ϵ_F , and the corresponding ground state solution is the same as obtained in the natural basis.

Consider now the following representation of

$$Q(\epsilon) = \begin{pmatrix} (\epsilon - E)^{1/2} & 0 & 0 & 0 \\ 0 & I & 0 & 0 \\ 0 & 0 & I & 0 \\ 0 & 0 & 0 & I \end{pmatrix} \begin{pmatrix} I & 0 & \alpha & \alpha \\ 0 & P & P & 0 \\ \alpha & P & P & F \\ \alpha & 0 & F & F \end{pmatrix} \begin{pmatrix} (\epsilon - E)^{1/2} & 0 & 0 & 0 \\ 0 & I & 0 & 0 \\ 0 & 0 & I & 0 \\ 0 & 0 & 0 & I \end{pmatrix}, \quad (\text{A3})$$

we recognize that the $\alpha = (\epsilon - E)^{-1/2}F$ matrices are negligible to order $E^{-1/2}$ below ϵ_F . Thus, the two sets of functions do not mix up and the solution for the ground state in the common basis is the same as in the natural basis.

The difference matrix $V = Q^f - Q$ has the structure:

$$V = \begin{pmatrix} F - \epsilon + E & 0 & 0 & 0 \\ 0 & \epsilon - E - P & -P & 0 \\ 0 & -P & F - P & 0 \\ 0 & 0 & 0 & 0 \end{pmatrix}_{A',A,B,D} \quad (\text{A4})$$

Since Eq. (4) of Sec. II is satisfied, we can proceed formally as in that section and obtain, after defining $(F')_{A',B} = [(G^f)_{A',B}]^{-1}$:

$$G_C = [(G_C^f)^{-1} - V_C]^{-1} = \begin{pmatrix} F' - F - E + \epsilon & 0 & F' \\ 0 & P & P \\ F' & P & F' + P - F \end{pmatrix}_{A',A,B} \quad (\text{A5})$$

Again, due to the presence of the E term in the diagonal A' block, this equation factorizes into an inessential equation for the subcluster A' and Eq. (21) for the cluster $A \cup B$.

$\hat{Q} = \hat{G}^{-1}$ in the common basis:

$$Q(\epsilon) = \begin{pmatrix} \epsilon - E & 0 & F & F \\ 0 & P & P & 0 \\ F & P & P & F \\ F & 0 & F & F \end{pmatrix}_{A',A,B,D} \quad (\text{A2})$$

Here $Q(\epsilon)$ coincides with the usual representation of $\hat{Q}(\epsilon)$ in the subset $A \cup B \cup D$, P standing for perturbed and having assumed that $H_{AD} = 0$, $H_{BD} = H_{BD}^f$, $H_D = H_D^f$ [assumption (a')]. The Q matrix does not factorize into two diagonal blocks since the submatrices $Q_{A',D}$ are nonzero; its resulting structure is exactly the same as that of the matrix introduced by Bernholc *et al.*¹⁴ After writing:

APPENDIX B

Consider a transformation between a set of orthogonalized atomic orbitals χ_μ , as used in CNDO, and a set of hybrid atomic orbitals:

$$t_\rho = \sum_\mu v_{\rho\mu} \chi_\mu \quad (\text{B1})$$

The V matrix is a block diagonal matrix, each submatrix V_A along the diagonal having the size of the basis on atom A . In our case:

$$V_A = \begin{pmatrix} 1/\sqrt{3} & (2/3)^{1/2} & 0 & 0 \\ 1/\sqrt{3} & -1/\sqrt{6} & 1/\sqrt{2} & 0 \\ 1/\sqrt{3} & -1/\sqrt{6} & -1/\sqrt{2} & 0 \\ 0 & 0 & 0 & 1 \end{pmatrix} \quad (\text{B2})$$

Due to the orthogonality of the set $\{\chi\}$, we have:

$$\langle t_\rho | t_\sigma \rangle = S_{\rho\sigma} = (V\tilde{V})_{\rho\sigma} \quad (\text{B3})$$

In the new basis the density matrix becomes:

$$P' = \tilde{V}^{-1} P V^{-1} \quad (\text{B4})$$

and according to a Mulliken population analysis, the electron population that can be attributed to the hybrid orbital t_ρ on atom A is:

$$n_\rho = \sum_\sigma P'_{\rho\sigma} S_{\sigma\rho} = (\tilde{V}^{-1} P \tilde{V})_{\rho\rho} = (\tilde{V}_A^{-1} P_A \tilde{V}_A)_{\rho\rho} \quad (\text{B5})$$

- ¹R. Haydock, V. Heine, and M. J. Kelly, *J. Phys. C* **5**, 2845 (1972).
- ²F. Cyrot-Lackmann, *J. Phys. (Paris) Suppl. C* **1**, 67 (1970); F. Cyrot-Lackmann and F. Ducastelle, *Phys. Rev. B* **4**, 2406 (1971).
- ³T. B. Grimley, in *Proceedings of the International School of Physics Enrico Fermi, Course LVIII*, edited by F. Goodman (Compositori, Bologna, 1974), p. 298.
- ⁴C. Weigel, S. T. Chui, and J. W. Corbett, *Phys. Rev. B* **18**, 2377 (1978).
- ⁵A. K. Gupta, P. Jena, and K. S. Singwi, *Phys. Rev. B* **18**, 2712 (1978).
- ⁶G. T. Surratt and W. A. Goddard III, *Phys. Rev. B* **18**, 2831 (1978).
- ⁷A. B. Kunz and D. L. Klein, *Phys. Rev. B* **17**, 4614 (1978).
- ⁸A. Zunger and R. Englman, *Phys. Rev. B* **17**, 642 (1978).
- ⁹S. G. Louie, M. Schlüter, L. Chelikowsky, and M. L. Cohen, *Phys. Rev. B* **13**, 1634 (1976).
- ¹⁰G. D. Watkins and R. P. Messmer, *Phys. Rev. Lett.* **25**, 656 (1970); *Phys. Rev. B* **7**, 2568 (1973); C. Weigel, D. Peak, J. W. Corbett, G. D. Watkins, and R. P. Messmer, *ibid.* **8**, 2906 (1973).
- ¹¹T. B. Grimley and E. E. Mola, *J. Phys. C* **7**, 2831 (1974).
- ¹²A. Zunger, *J. Chem. Phys.* **63**, 1713 (1975).
- ¹³G. F. Koster and J. C. Slater, *Phys. Rev.* **95**, 1167 (1954). J. Callaway, *J. Math. Phys.* **5**, 783 (1964).
- ¹⁴S. T. Pantelides, J. Bernholc, J. Pollman, and N. O. Lipari, *Int. J. Quantum Chem.* **S12**, 507 (1978).
- ¹⁵J. Bernholc and S. T. Pantelides, *Phys. Rev. B* **18**, 1780 (1978).
- ¹⁶J. Bernholc, N. O. Lipari, and S. T. Pantelides, IBM Thomas J. Watson Research Center, Report No. RC 7261 (unpublished).
- ¹⁷T. B. Grimley and C. Pisani, *J. Phys. C* **7**, 2831 (1974).
- ¹⁸R. A. Van Santen and L. H. Toneman, *Int. J. Quantum Chem.* **12**, Suppl. 2, 83 (1977).
- ¹⁹C. Pisani, *Phys. Rev. B* **17**, 3143 (1978).
- ²⁰O. Gunnarsson and H. Hjelmberg, *Phys. Scr.* **11**, 97 (1975).
- ²¹O. Gunnarsson, H. Hjelmberg, and B. I. Lundquist, *Surf. Sci.* **63**, 348 (1977).
- ²²H. Hjelmberg (unpublished).
- ²³J. A. Pople and D. L. Beveridge, *Approximate Molecular Orbital Theory* (McGraw-Hill, New York, 1970).
- ²⁴C. Pisani and R. Dovesi, *Int. J. Quantum Chem.* (to be published).
- ²⁵R. Dovesi, C. Pisani, and C. Roetti, *Int. J. Quantum Chem.* (to be published).
- ²⁶D. J. Chadi, *Phys. Rev. B* **16**, 3572 (1977).
- ²⁷J. L. Fry, N. E. Brener, and R. K. Bruyère, *Phys. Rev. B* **16**, 5225 (1977).
- ²⁸A. J. Bennett, B. Mc Carroll, and R. P. Messmer, *Phys. Rev. B* **3**, 1397 (1971).
- ²⁹W. N. Reynolds, *Physical Properties of Graphite* (Elsevier, Amsterdam, 1968).